Available online at www.sciencedirect.com

SCIENCE DIRECT®

Magnetic Resonance Imaging 23 (2005) 295–299

MAGNETIC RESONANCE IMAGING

NMR in rotating magnetic fields: magic-angle field spinning

Dimitris Sakellariou[a,b,c], Carlos A. Meriles[a,b,d], Rachel W. Martin[a,b], Alexander Pines[a,b,*]

[a]*Materials Sciences Division, Lawrence Berkeley National Labs, Berkeley, CA 94720, USA*
[b]*Department of Chemistry, University of California, Berkeley, CA 94720, USA*
[c]*CEA, Saclay, DSM/DRECAM/ Service de Chimie Moléculaire, F-91191 Gif-sur-Yvette Cedex, France*
[d]*Physics Department, City College of New York (CUNY), New York, NY 10031, USA*

Abstract

Magic-angle sample spinning is one of the cornerstones in high-resolution NMR of solid and semisolid materials. The technique enhances spectral resolution by averaging away rank 2 anisotropic spin interactions, thereby producing isotropic-like spectra with resolved chemical shifts and scalar couplings. In principle, it should be possible to induce similar effects in a static sample if the direction of the magnetic field is varied (e.g., magic-angle rotation of the B_0 field). Here we will review some recent experimental results that show progress toward this goal. Also, we will explore some alternative approaches that may enable the recovery of spectral resolution in cases where the field is rotating off the magic angle. Such a possibility could help mitigate the technical problems that render difficult the practical implementation of this method at moderately strong magnetic fields.

Keywords: Rotating field; Magic-angle spinning; Averaging; High resolution; Ex situ NMR; HR-MAS; Susceptibility broadening

1. Introduction

High-resolution NMR of anisotropic samples is typically performed by spinning a sample at the magic angle (54.7°). In modern solid-state NMR, the combination of sample spinning and high-power multiple-pulse decoupling has led to the development of sophisticated analytical techniques that result in a tremendous resolution enhancement [1]. In "liquid-state" NMR of semisolid or hydrated samples, the application of MAS to average magnetic susceptibility had great success to the extent that the technique gained its own name, "HR-MAS". Applications of HR-MAS to biological samples showed that the resolution enhancement was such that new medical problems could be tackled [2]. MAS was also combined with magnetic field gradients allowing for magnetic resonance imaging of solid objects [3].

There are situations, however, where the physical manipulation of the sample turns out to be inconvenient or even impossible. Living subjects are a clear example (despite the fact that even a slow rotation can lead to a remarkable resolution enhancement [4–6]). Another such case is ex situ NMR where, by definition, a static sample outside the confines of the magnet must be probed. An elegant, although experimentally demanding, solution to this problem was proposed by Andrew and Eades [7] in an early theoretical work. In the adiabatic limit, the frequency of the field rotation is slower than the Larmor frequency of the nuclei so that spins follow the motion of the field at all times during their evolution. This idea has been analyzed and extended to generalized field trajectories and pulse sequences within the context of zero-field NMR and dipolar time-reversal echoes [8]. A more recent implementation has been used to study Berry's phase after a 2π rotation of the field and has led to the development of an NMR-based gyroscope [9]. Field rotation at the magic angle has also been combined with field cycling to study the dynamics of liquid crystals [10].

In this paper, we will first outline how field spinning operates on different spin interactions. Then, we will briefly review recent experimental results that illustrate this methodology and show that, in principle, a high-resolution spectrum can be obtained even if the spinning angle differs from the magic angle. Finally, we will discuss some possibilities for the practical implementation of magnetic field rotation at moderately high magnetic fields.

* Corresponding author.
E-mail address: pines@berkeley.edu (A. Pines).

0730-725X/$ – see front matter © 2005 Elsevier Inc. All rights reserved.
doi:10.1016/j.mri.2004.11.067

2. Spin evolution in the presence of a rotating magnetic field

Consider a rotating magnetic field consisting of a time-independent component along the z-axis of the laboratory frame and two oscillating components in the xy plane [see Fig. 1(A)]:

$$B(t) = B_{xy}\left[\cos(\omega_r t)\hat{u}_x + \sin(\omega_r t)\hat{u}_y\right] + B_z\hat{u}_z \quad (1)$$

The Hamiltonian of a nuclear spin I subject to this magnetic field is also time dependent:

$$H(t) = -\mu\cdot B(t) = \gamma_I B_{xy}\left[\cos(\omega_r t)I_x + \sin(\omega_r t)I_y\right] + \gamma_I B_z I_z \quad (2)$$

Using an interaction rotating frame defined by the rotation transformation $V_1(t)=\exp(+i\omega_r t I_z)$ followed by a second tilted frame transformation $V_2=\exp(+i\theta I_y)$ with θ defined by

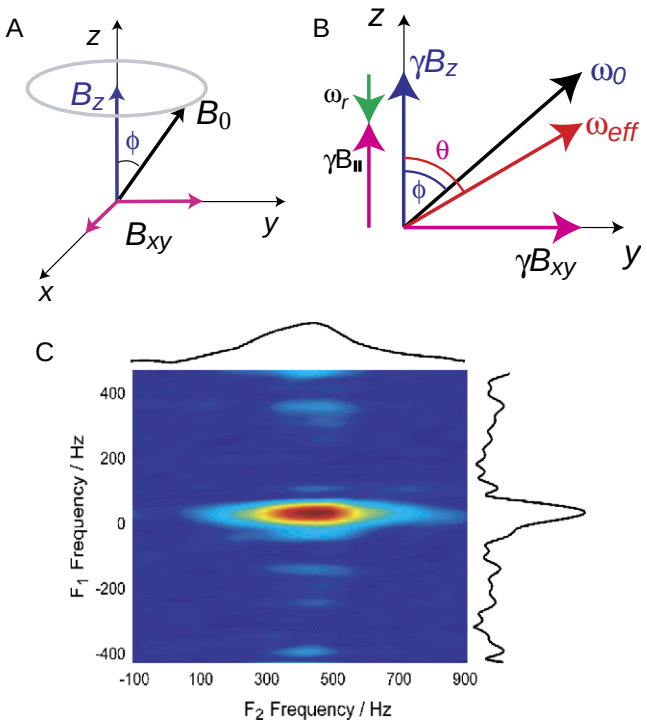

Fig. 1. (A) Rotating magnetic field in the laboratory frame. (B) Schematic diagram defining the angles θ and ϕ for the components of the effective Hamiltonian in the rotating frame of $V_1(t)$. (C) Anisotropic – isotropic chemical shift correlation spectrum in a static sample of hyperpolarized solid xenon obtained by field rotation at the magic angle. The acquisition dimension F_2 (labeled on plot) displays the full dipolar broadening observed when the field remains static (FWHM~350 Hz). This broadening is substantially reduced during the evolution dimension F_1 by making the field describe a conical trajectory at the magic angle prior to acquisition. In this case, the projection along F_1 exhibits a residual broadening of only ~60 Hz primarily due to experimental imperfections. The field strength was ~34 G during field spinning and was reduced to ~21 G during acquisition. The field-spinning rate was 2 kHz. Notice the absence of sidebands in the narrowed spectrum due to the rotor synchronization imposed by the chosen sampling time (2 rotations per point in the indirect dimension). Adapted from Ref [11].

$\theta = \arctan\frac{\gamma_I B_{xy}}{\gamma_I B_z - \omega_r}$ [see also Fig. 1(B)], the previous Hamiltonian can be written in a form where it is diagonal and time independent:

$$H_2 = V_2 V_1(t) H(t) V_1^{-1}(t) V_2^{-1} = \omega_{\text{eff}} I_z. \quad (3)$$

The effective Larmor frequency is then:

$$\omega_{\text{eff}} = \sqrt{(\gamma_I B_z - \omega_r)^2 + (\gamma_I B_{xy})^2}. \quad (4)$$

Under magic-angle field spinning, the Hamiltonian governing chemical shifts and dipolar or quadrupolar interactions in the laboratory frame is given by:

$$H(t) = -\mu\cdot B(t) + \sum_{\lambda} H_\lambda \quad (5)$$

where each interaction Hamiltonian [1] can be written as $H_\lambda = \sum_l \sum_{m=-l}^{l} (-1)^m R^{\lambda}_{l,-m} T_{l,m}$.

If we perform the previous transformations $V_1(t)$ and V_2, the final effective nontruncated Hamiltonian is:

$$\tilde{H}_\lambda = \sum_l \sum_{m,\text{n}} (-1)^m D_m d^{(l)}_{n,-\text{m}}(\theta) e^{-i(m\omega_r + n\omega_{\text{eff}})t} T_{l,\text{n}} \quad (6)$$

When the rotation rate is stronger than the magnitude $\|H_\lambda\|$ of the interaction, it is permissible to truncate the Hamiltonian along the effective field[1]. Then the secular part corresponds to $n=0$ and reads:

$$\bar{H}_\lambda = \sum_l \sum_m (-1)^m D_m d^{(2)}_{0,-m}(\theta) e^{-im\omega_r t} T_{l,0} \quad (7)$$

$d^{(l)}_{n,m}$ are the Wigner matrix elements of the transformation. If we define the isotropic scaling factor as the ratio between the rotating field chemical shift and the isotropic shift in a static field, then, after some algebra, one finds:

$$\lambda_{\text{iso}} = 1 + \frac{\omega_r}{\omega_{\text{eff}}}\cos\theta \quad (8)$$

for the isotropic part of the chemical shift and

$$\lambda_{\text{aniso}} = \frac{\omega_0}{\sqrt{6}\omega_{\text{eff}}}[3\cos\theta\cos\phi - \cos(\theta-\phi)] \quad (9)$$

for the anisotropic part. In the adiabatic limit, where the spinning frequency is small compared with the field components, we have $\theta\approx\phi$ and the scaling factors reduce to:

$$\lambda_{\text{iso}} = 1,\ \lambda_{\text{aniso}} = 3\cos^2\theta - 1 \quad (10)$$

meaning that only the isotropic chemical shift remains if we spin at the magic angle: $\phi=\theta_{\text{m}}$. Finally, assuming that the spinning frequency is large enough and no recoupling conditions are met, we obtain for the dipolar contribution:

$$\bar{H}_D = D_{20} d^{(2)}_{0,0}(\theta) T_{2,0} \quad (11)$$

which vanishes if $\theta=\theta_{\text{m}}$ even if the rotation is nonadiabatic.

[1] One has to be careful about recoupling conditions that can occur under rotation synchronization since the truncation will not lead to the same average Hamiltonian.

3. Practical implementations of field spinning

The first experimental demonstration of the use of field rotation to average anisotropic interactions was performed recently [11] and is shown in Fig. 1(C). In this particular case, field spinning is used to reduce the dipolar broadening in a spectrum of solid hyperpolarized ^{129}Xe. Three orthogonal Helmholtz pairs are used to set the field direction. Throughout the experiment, one of the pairs provided a constant field of ~21 G. The other two pairs were driven via two current amplifiers. To avoid saturating the receiver, a 2D scheme that probed the evolution of the magnetization during rotation point-by-point-wise while the field direction was changing was implemented. In the direct dimension (F_2), the spectrum displays the full dipolar broadening of solid ^{129}Xe, which is ~350 Hz. To a large extent, this is removed by magic-angle field spinning: the line width in the indirect (F_1) dimension has narrowed down to ~60 Hz, approximately 1/6 of the anisotropic line width.

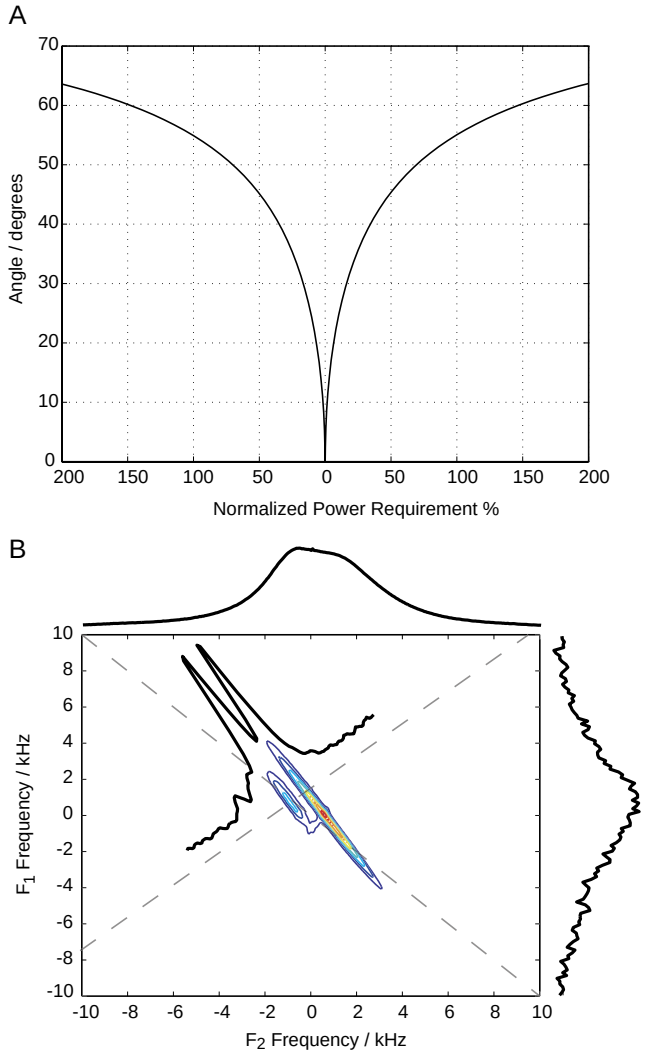

Fig. 2. (A) Diagram representing the relative power requirements necessary to obtain electromagnetic field spinning at a given rotation angle. The normalization is made assuming that 100% is the power needed at the magic angle. From the diagram one can appreciate the sharp drop in power requirements when the angle is close to zero. (B) Two-dimensional p-MAS spectrum of a sample containing glass beads saturated with water and mineral oil. The angles θ_1 and θ_2 were set at 4.5 and 25 degrees respectively. The experimental scaling factor was 0.15. Adapted from Ref [12].

Although this example nicely illustrates the potential feasibility of the magic-angle rotation of the B_0 field, its application to truly interesting situations still depends on our ability to manipulate the direction of moderately strong magnetic fields because of the need for enhanced sensitivity and chemical shift resolution. For the case in which field rotation is performed by modulating the source currents, the practical implementation of this method automatically becomes demanding because the power required rapidly grows with the magnetic field magnitude. One interesting question is, however, whether attaining the magic angle during the field trajectory is absolutely necessary. This question is motivated by the observation that, for a given field magnitude, the relative power required to cycle the field direction sharply depends on the angle of the cone described. Notice that, as shown in Fig. 2(A), only ~15% of the original power is needed if the angle is set, for instance, at 20°.

Recently, a method capable of providing a high-resolution isotropic spectrum at two angles different from the magic angle has been introduced [12]. In this scheme, called projected MAS or p-MAS, spins evolve under two different angles, θ_1 and θ_2, during times t_1 and t_2 in a 2D experiment. The result is a 2D spectrum that correlates two anisotropic dimensions each having a width determined by the values of the respective second-order Legendre polynomials evaluated at θ_1 and θ_2. Nevertheless, resolution is recovered with an appropriate projection or "shearing" that produces isotropic chemical shifts scaled by a scaling factor. The slope of the projection depends on the ratio of the two polynomials for the two angles.

A model spectrum recorded at high field is shown in Fig. 2(B). The sample chosen, which has been previously used as a model for susceptibility broadening in living tissues [4–6], was prepared by soaking with mineral oil and water 100- to 200-μm-diameter glass beads packed in a rotor. Inside a magnetic field of 11.2 T, the static spectrum has a line width of 7 kHz, while the residual broadening under MAS is 80 Hz. The angles were set at θ_1=4.5° and θ_2=26°, providing a theoretical scaling factor of 0.16 for the isotropic chemical shift. After a shearing transformation, one can obtain a trace displaying the isotropic spectrum as shown. The two resonances from water (left) and mineral oil (right) can be clearly distinguished. This technique has been also successfully demonstrated in living tissue samples [13] giving an important resolution enhancement.

Another possibility is the use of a well-known method called variable angle correlation spectroscopy (VACSY), which is based on the acquisition of independent 1D spectra for a range of rotation angles [14]. Unlike in the method described before, no (fast) angle switching is required, so the

field spinning can be stabilized before each data acquisition. For electromagnetic and/or mechanical field rotation, small variations of the spinning angle around 0° (or around 90°) would facilitate tremendously the construction and operation of such magnets.

At a given angle, the signal has an isotropic and an anisotropic part. On a 2D reference frame where each of these components is made orthogonal, each FID can be plotted along a direction that depends on the rotation angle. After a 2D Fourier transform in this frame, a correlation between the isotropic and anisotropic parts of the chemical shift tensor is obtained. For the traditional high-field sample spinning VACSY, the sampled angles are not constrained. However, if the signal to noise is adequate, even a small set of spectra recorded at small angles [see Fig. 3(C)] would suffice to reconstruct the isotropic spectrum. Singular value decomposition [15] may be used to reconstruct the (missing) isotropic spectrum. Then a Fourier transform along the other dimension should give us the anisotropic part of the interactions.

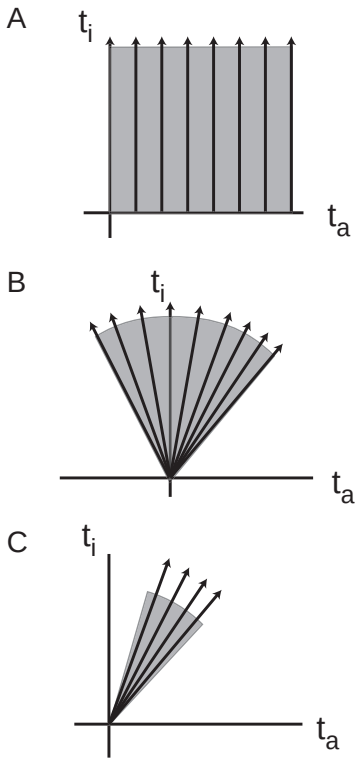

Fig 3. Schematic diagram of k space data acquisition in standard 2D NMR and VACSY. (A) In standard 2D data are acquired during t_a for each value of the indirect evolution time t_i. A Cartesian two-dimensional FID signal grid is formed and processed using 2D FT. (B) In VACSY the data are acquired during time t for each value of the spinning angle. The acquired data do not have an equidistant spacing in k space and interpolation onto a Cartesian grid is necessary. In principle the data cover a large two-dimensional area since the angle can vary from 0 to 90 degrees. (C) In limited-VACSY only a small part of the 2D plane is covered and data prediction is needed in order to recover the lost information.

The use of either one of these two approaches may result in the development of methods using off-magic-angle rotation of stronger magnetic fields. Spinning at small angles would allow a stronger magnetic field to be rotated using the same amount of power, resulting in greater sensitivity and resolution. However, before useful field rotation experiments can be performed, several technical obstacles remain to be overcome. The first one is the necessity of rotating the field much more slowly than the spinning rates (typically several kilohertz) used in standard sample spinning experiments such as those described here. Slow-spinning versions of p-MAS and VACSY, based on a magic angle turning experiment [4–6], are currently under development.

At this point in the evolution of field spinning methods, it is not clear whether it is more convenient to rotate the field electromagnetically or mechanically. Electromagnetic rotation provides greater freedom in conceivable field trajectories, but the rotation frequency and angle switching speed are limited by the inductance of the coils used. Another possibility is mechanical rotation of a permanent magnet [16], either on its own or in conjunction with an electromagnetic field of variable angle. In this approach, the field trajectory and RF pulsing could be synchronized to emulate a magic angle turning-type approach. This method could be particularly interesting because it may enable the use of ultraslow spinning rates that have been successfully used to remove susceptibility broadening in samples of biological tissue [4–6].

Despite the early insight of Andrew and Eades [7] that spinning the magnetic field is equivalent to spinning the sample to remove anisotropic interactions, only limited experimental realizations have thus far been performed. This is because of the stringent requirements for power, heat dissipation, rotation frequency and field homogeneity. In this paper, we reviewed the principles of field spinning as well as some potential methods for relaxing these experimental constraints. Solid-state NMR turning experiments provide a means to correlate isotropic and anisotropic interactions under a sample rotation frequency much smaller than the size of the interaction. Turning-sample experiments can be, in principle, adapted for turning magnetic fields, allowing the use of methods currently restricted to the fast-spinning regimen of modern solid-state NMR. Small-angle methods such as p-MAS and limited VACSY allow recovery of isotropic spectra under the small spinning angles easily accessible to rotating fields, allowing stronger fields to be used, based on electromagnetic and/or mechanical field rotation.

References

[1] Haeberlen U. High resolution NMR in solids: selective averaging. In: Waugh JS, editor. Advances in Magnetic Resonance, Suppl, Vol 1. New York: Academic Press; 1976. p. 37–91.

[2] Cheng LL, Ma MJ, Becerra L, Ptak T, Tracey I, Lackner A, et al. Quantitative neuropathology by high resolution magic angle spinning proton magnetic resonance spectroscopy. Proc Natl Acad Sci USA 1997;94:6408.

[3] Blümich B. NMR imaging of materials. Oxford: Oxford Science Publications, Clarendon Press; 2000.
[4] Wind RA, Hu JZ, Rommerein DN. High-resolution ^{1}H NMR spectroscopy in organs and tissues using slow magic angle spinning. Magn Reson Med 2001;46:213.
[5] Wind RA, Hu JZ, Rommerein DN. High-resolution ^{1}H NMR spectroscopy in a live mouse subjected to 1.5 Hz magic angle spinning. Magn Reson Med 2003;50:1113.
[6] Hu JZ, Rommereim DN, Wind RA. High-resolution ^{1}H NMR spectroscopy in rat liver using magic angle turning at a 1 Hz spinning rate. Magn Reson Med 2002;47:829.
[7] Andrew ER, Eades RG. Possibilities for high-resolution nuclear magnetic resonance spectra of crystals. Discuss Faraday Soc 1962; 34:38.
[8] Lee CJ, Suter D, Pines A. Theory of multiple-pulse NMR at low and zero fields. J Magn Reson 1987;75:110.
[9] Härle P, Wäckerle G, Mehring M. A nuclear-spin based rotation sensor using optical polarization and detection methods. App Magn Reson 1993;5:207.
[10] Noack F, St. Becker S, Struppe J. Applications of field-cycling NMR. Annu Rep NMR Spectrosc 1997;33:1.
[11] Meriles CA, Sakellariou D, Moulé A, Goldman M, Budinger T, Pines A. High-resolution NMR of static samples by rotation of the magnetic field. J Magn Reson 2004;169:13.
[12] Sakellariou D, Meriles CA, Martin RW, Pines A. High-resolution NMR of anisotropic samples with spinning away from the magic angle. Chem Phys Lett 2003;377:333.
[13] Martin RW, Jachmann RC, Sakellariou D, Nielsen UG, Pines A. High-resolution NMR of biological tissues using projected magic angle spinning. Magn Reson Med 2005 [in press].
[14] Frydman L, Chingas GC, Lee YK, Grandinetti PJ, Eastman MA, Barrall GA, et al. Variable-angle correlation spectroscopy in solid-state nuclear magnetic resonance. J Chem Phys 1992;97:4800.
[15] Lin Y-Y, Hodgkinson P, Ernst M, Pines A. A novel detection–estimation scheme for noisy NMR signals: applications to delayed acquisition data. J Magn Reson 1997;128:30.
[16] Moresi G, Magin R. Miniature permanent magnet for table-top NMR. Concepts Magn Reson 2003;19B:35.